Stream-Discharge Surges Generated by Groundwater Flow

Adrien Guérin, Olivier Devauchelle, Vincent Robert, Thierry Kitou, Céline Dessert, Amélie Quiquerez, Pascal Allemand, Éric Lajeunesse

Stream-discharge surges generated by groundwater flow

Adrien Guérin[1], Olivier Devauchelle[1], Vincent Robert[1], Thierry Kitou[1], Céline Dessert[1], Amélie Quiquerez[2], Pascal Allemand[3], and Eric Lajeunesse[1]

[1]Institut de Physique du Globe de Paris, Sorbonne Paris Cité, Université Paris Diderot, UMR 7154 CNRS, 1 rue Jussieu, 75238 Paris, Cedex 05, France
[2]Université de Bourgogne, UMR CNRS 6298, ARTeHIS, 6 Boulevard Gabriel, 21000 Dijon, France
[3]Université Claude Bernard Lyon 1, Ens de Lyon, CNRS, UMR 5276 LGL-TPE, F-69622, Villeurbanne, France

Key Points:

- High-frequency measurements show that groundwater non-linearly amplifies the response of a catchment to rainfall events.
- The storm-flow regime of the underground flow consistently predicts the peak runoff.
- We propose a method to measure the available volume of groundwater stored in a shallow aquifer based on its catchment's hydrograph.

Corresponding author: Olivier Devauchelle, `devauchelle@ipgp.fr`

Abstract

Catchments respond to rainfall by storing and releasing water according to their internal dynamics. Groundwater had long been treated as the slow reservoir in this process, but isotopic measurements showed how responsive it can be. Here, we investigate the mechanics of groundwater's contribution to floods. To do so, we monitored over three years the shape of the water table in, and the runoff out of, a small tropical catchment. We find that groundwater and runoff respond within minutes of a rainfall event. Using an asymptotic theory inspired by recent laboratory experiments, we suggest that the peak water discharge at the catchment's outlet increases like the rainfall rate to the power of 3/2. This formula consistently predicts the stream's response to the 137 isolated rainfall events recorded during our field survey. In addition, its prefactor yields an estimate of the average groundwater storage.

Plain Language Summary Rainwater infiltrates into the ground, accumulates in porous rocks, and eventually flows towards a neighboring stream. Although this underground travel often takes millennia, groundwater can contribute quickly to floods. To understand how an underground flow can be so responsive, we have recorded the motion of the groundwater surface in a small tropical catchment during three years. We find that groundwater swells within minutes of a rain event, and that this deformation directly pushes more water into the stream. The resulting stream-discharge peak strengthens faster than the rainfall intensity: a three-fold increase of the latter causes a five-fold increase of the stream discharge. Including this mechanism into flood-forecasting models should allow us to better predict the impact of extreme precipitations. Finally, we introduce a method to measure how much water an aquifer stores during a rainfall event, before releasing it—a central parameter for the management of water resources.

1 Introduction

The typical hydrograph of a river draining a small catchment (i.e. the time series of its discharge) increases steeply during rainfall, and declines slowly afterward, as groundwater reservoirs empty into the drainage system (Sefton, Whitehead, Eatherall, Littlewood, & Jakeman, 1995). Catchments thus shape their response to rainfall by storing water, and then releasing it into the network of streams that drains them (Harman & Sivapalan, 2009; Kirchner, 2009). Understanding this process is a formidable task: before it reaches a stream, rainwater infiltrates into the vadose zone (Maher, DePaolo, Conrad, & Serne, 2003), is absorbed by the roots of trees (Mares, Barnard, Mao, Revil, & Singha, 2016), and eventually joins the groundwater zone, where it flows through heterogeneous and fractured rocks (Berkowitz, 2002; De Marsily et al., 2005; Goderniaux, Davy, Bresciani, Dreuzy, & Le Borgne, 2013). There is little doubt that it is groundwater that sustains the recession limb of a hydrograph after a rainfall event (Brutsaert & Nieber, 1977). During the event itself, however, the significance of its contribution to the rising limb of the hydrograph remains debated (Kirchner, 2003). Most streams remain chemically close to groundwater even at their peak discharge, indicating that groundwater can respond quickly to rainfall (Jasechko, Kirchner, Welker, & McDonnell, 2016; McDonnell, 2003; Neal & Rosier, 1990; M. Sklash, 1990). For this to happen, the vadose zone must promptly transmit the rainfall signal to the water table, but the mechanisms by which it does so remain controversial (McDonnell et al., 2010). Likely candidates include water flowing through non-capillary cracks (Beven & Germann, 1982; McDonnell, 1990; McGlynn, McDonnel, & Brammer, 2002; Tromp-van Meerveld & McDonnell, 2006), and ridging in the capillary fringe (Abdul & Gillham, 1984; Cloke, Anderson, McDonnell, & Renaud, 2006; Fiori, Romanelli, Cavalli, & Russo, 2007; M. G. Sklash & Farvolden, 1979).

Once it reaches the water table, rainwater raises the pressure in the groundwater zone. How the water table responds to this change in the pressure field, and ultimately pushes

water into the drainage network, depends on the aquifer's geometry. In steep and shallow aquifers, the rainfall signal travels as a kinematic wave driven by gravity (Beven, 1981; Tani, 1997). In more typical aquifers, however, it is the pressure gradient that drives the flow through the porous rock. In general, one then needs to consider both the horizontal and vertical components of the groundwater flow which, in steady state, determine the flow pattern and the distribution of the transit time through the aquifer (Cardenas, 2007; Toth, 1963). Dynamical simulations in unconfined aquifers prove more challenging.

When permeability decreases steeply with depth, or when an impervious horizon bounds the groundwater flow, the latter is mostly horizontal, and one can combine Darcy's law to the shallow-water approximation to derive the Boussinesq equation (Boussinesq, 1904; Dupuit, 1848). Brutsaert and Nieber (1977) used this equation, in its original non-linear form, to estimate the hydraulic properties of an unconfined aquifer based on the recession limb of its hydrograph. This method, and the associated power-law of the recession limb, has since become a staple of groundwater hydrology (Troch et al., 2013, and references therein).

Only recently, however, has the Boussinesq equation been invoked to represent the rising limb of a hydrograph (Pauwels & Troch, 2010). Based on numerical solutions of the linearized Boussinesq equation, Fiori (2012) showed that it could simulate a complete hydrograph, and explain the chemical composition of the groundwater that feeds a stream during a rainfall event. Pauwels and Uijlenhoet (2019) confirmed the validity of this equation in gently sloping laboratory aquifers submitted to a sudden rainfall event, showing that unconfined aquifers react virtually instantly to a rainfall input. These results, however, must be reconciled with the power-law recession of the hydrograph, which can result only from the non-linear Boussinesq equation. Laboratory experiments achieve this reconciliation when the aquifer's outlet, which represents a stream, coincides whith the impermeable base of the aquifer (Guérin, Devauchelle, & Lajeunesse, 2014). In this configuration, the flow can enter a new asymptotic regime (the "storm-flow regime"), during which the aquifer's discharge increases in proportion to $R_s^{3/2}$, where R_s is the recharge rate.

If it occurs in nature, this non-linear regime would especially amplify the most intense rainfall events. To our knowledge, however, it has never been identified in the field. Here, we combine high-frequency field measurements with the classical Boussinesq approximation to seek out the storm-flow regime in a small catchment.

2 Field Setup

To identify the storm-flow regime in a natural setting, we instrumented an eight-hectare catchment in the volcanic island of Basse-Terre, in the Guadeloupe archipelago, French West Indies (Figure 1a). There, the pristine forest of the Guadeloupe National Park covers an at least 10 m-thick layer of unconsolidated clay (Buss et al., 2010; Clergue et al., 2015) (Figure 1b), the hydraulic conductivity of which typically ranges from about 10^{-6} to $10^{-5}\,\mathrm{m\,s^{-1}}$ depending on compaction and composition (Colmet-Daage & Lagache, 1965, Supporting Information Text S1). An electrical resistivity tomography survey revealed a homogeneous aquifer, with no visible horizon in the clay layer (Supporting Information Text S1 and Figure S1). This shallow catchment (its surface slope is 14° on average) is drained by the Quiock creek, a stream less than 2 m wide. Outside this stream and its tributaries, the catchment shows no indication of surface runoff—the ground is permanently littered with decaying leaves.

Modern pressure transducers can record high-frequency measurements over months without human intervention, making it possible to monitor accurately the response of groundwater to a long series of rainfall events. We installed eight such transducers in the Quiock catchment, seven of which in piezometric wells arranged in a linear array which extends, perpendicularly to the stream, over 30 m (Figure 1c). This disposition allows us to

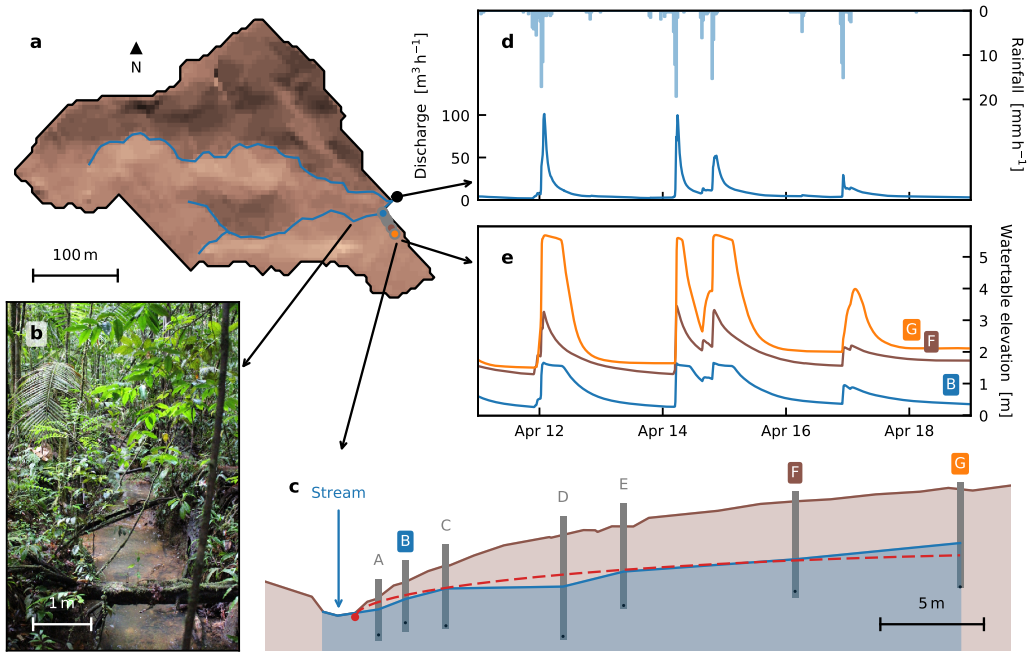

Figure 1. Instrumented catchment of the Quiock creek, Guadeloupe, French West Indies. (a) Map of the catchment (16° 10′ 36″ N, 61° 41′ 44″ W). Dots indicate piezometric wells. (b) Quiock creek about 10 m upstream of measurements. (c) Cross section of the shallow aquifer. Blue line shows the root mean square of the water table profile, h_{RMS}, from January 2015 to October 2017. Red dashed line corresponds to equation (1). Brown shaded area, grey lines and black dots indicate ground surface, boreholes and pressure sensors respectively. (d) Time series of the stream discharge and rainfall rate (April 2015). (e) Time series of the water-table elevation, with respect to stream level, at 2.4, 21 and 29 m from the river.

reconstruct the shape of the groundwater surface every minute. We placed the eighth transducer in a stream gauge to record the discharge of the Quiock creek at the same frequency. In addition, a tipping-bucket rain gauge measures precipitations less than 10 m away from the wells, below the canopy (Supporting Information Text S2).

3 Observations

We find that the Quiock catchment, like most catchments of its size, distorts the rain signal (Figure 1d). Right after the beginning of a rain event, the runoff increases quickly, sometimes tenfold within a few minutes. After the rain has stopped, the stream's discharge begins a recession that lasts until the next event, often days later.

Remarkably, although the groundwater surface lies a few meters below ground, it rises virtually instantly (Figure 1e), so much so that our measurements cannot tell which, of the groundwater or the stream, reacts first (Supporting Information Text S4 and Figure S2). This observation indicates that the pressure jump induced by fresh rainwater propagates through the vadose zone at a velocity of a few millimeters per second at least, before the water table responds to it. This fast transfer of the rainfall signal, common to many catchments (Abdul & Gillham, 1989; Sidle et al., 2000; Tromp-van Meerveld & McDonnell, 2006), remains the subject of active research (Cloke et al., 2006).

To interpret our observations, we first need to estimate the geometry and hydrological properties of the aquifer. We represent the former as simply as possible, by assuming that the groundwater flow is mostly orthogonal to the river. Accordingly, we estimate its horizontal extension L_a as half the average distance between two rivers, namely $L_a = A/(2L_r)$, where A is the area of the catchment, and L_r the total length of its drainage network. Based on the Lidar map of Figure 1a, we find $L_a \approx 40\,\mathrm{m}$.

We further assume (i) that there exists, at the catchment scale, a representative hydraulic conductivity K (Sanchez-Vila, Guadagnini, & Carrera, 2006), and (ii) that most of the groundwater flows horizontally in an active layer, above the stream elevation. If correct, these assumptions open the toolbox of the Boussinesq approximation: the pressure head in the aquifer is hydrostatic, and the Darcy flow it drives is induced by the local elevation of the water table (Boussinesq, 1904; Brutsaert & Nieber, 1977; Dupuit, 1848). Strictly speaking, approximation (ii) (often referred to as the "fully-penetrating stream") holds only when an impervious horizon joins the stream, and confines the groundwater flow above itself. We have no indication that such is the case in the Quiock catchment. One often finds, however, that the hydraulic conductivity of unconsolidated aquifers quickly decreases with depth, possibly due to compaction (McKay, Driese, Smith, & Vepraskas, 2005; Montgomery et al., 1997; Schoeneberger & Amoozegar, 1990). We expect that such a vertical gradient of conductivity would confine most of the flow to the layers lying above the stream. We cannot assess the validity of this point a priori; instead, we will deem it plausible as long as the catchment's behavior accords with it (Harman & Sivapalan, 2009). Asymptotic regimes, in particular, are sensitive to the physical mechanism that drives them (Barenblatt, 1996), and those of the Boussinesq equation would break down if the shallow-flow approximation were grossly inadequate. In the following, we interpret two of them as the signature of a shallow flow.

Averaging the Boussinesq equation over a sufficiently long period yields the textbook expression for the shape of a steady water table (Supporting Information Text S5):

$$h_{\mathrm{RMS}} = \sqrt{\frac{\langle R \rangle}{K}\, x\,(2\,L_a - x)} \tag{1}$$

where x is the distance to the stream, $\langle R \rangle$ is the average recharge rate and $h_{\mathrm{RMS}} = \sqrt{\langle h^2 \rangle}$ is the root mean square of the water table elevation. That h_{RMS} appears in the above equation, as opposed to the average elevation of the water table $\langle h \rangle$, results from the non-linearity of the Boussinesq equation (Eq. (2), Supporting Information Text S5). Here, we define h_{RMS} with respect to the stream's elevation, in accord with approximation (ii). Fitting the ratio $\langle R \rangle / K$ to our observations (Figure 1c), and estimating the recharge rate as the ratio of the average stream discharge to the area of the catchment, we find a catchment-scale hydraulic conductivity of $K = 5.6 \times 10^{-6}\,\mathrm{m\,s^{-1}}$, within the range of expected values for unconsolidated clay (Supporting Information Text S5).

Integrating h_{RMS} over the entire catchment yields an estimate of the aquifer volume that, on average, holds water above the stream's level :

$$V_r = \frac{\pi A L_a}{4} \sqrt{\frac{\langle R \rangle}{K}} \approx 1.9 \times 10^5\,\mathrm{m}^3\,. \tag{2}$$

This volume occupies a significant part of the available space in the aquifer, between the stream's level and the ground surface (Figure 1c). When rainfall reaches the water table, the aquifer's matrix gets refilled with water, in proportion to its fillable porosity ϕ_f—the ratio of the pore volume available to the rising water table to the total volume (Acharya, Jawitz, & Mylavarapu, 2012; Park & Parker, 2008; Sophocleous, 1991). Multiplying V_r with the fillable porosity thus yields an estimate of the volume of water, $V_a = \phi_f V_r$, that the aquifer stores above the stream's level, on average. In the framework of the Boussinesq approximation, this is the total volume of groundwater that, on average, would be released into the stream during a prolonged drought; we name it "available volume" on that account.

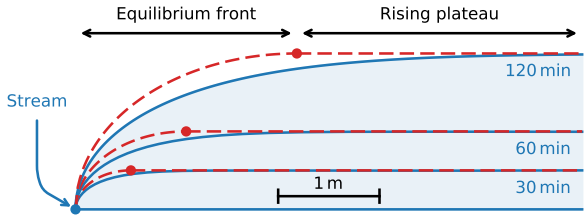

Figure 2. Theoretical shape of the water table during the storm-flow regime. For illustration, $R_s = 10\,\mathrm{mm\,h^{-1}}$, $\phi_f = 1.3 \times 10^{-2}$ and $K = 5.6 \times 10^{-6}\,\mathrm{m\,s^{-1}}$. Blue lines: self-similar solution of the Boussinesq equation (Guérin et al., 2014). Red dashed lines: approximate self-similar solution. Red dots indicate the transition between the equilibrium front and the rising plateau, at $x = L_f$.

Dividing this volume by the average discharge of the catchment yields a characteristic time, $T_c = V_a/\langle Q \rangle$ which, at this point, is merely a mathematical definition. We will see, however, that it will prove a convenient parameter to represent the reaction of the groundwater flow to a rainfall event.

We now use the recession of the water table after a rain to evaluate the validity of the Boussinesq approximation in the Quiock catchment, and to characterize its shallow aquifer (Rupp, Schmidt, Woods, & Bidwell, 2009; Troch et al., 2013). Once rainfall has stopped, the water table decreases in all piezometric wells, although at different rates, as the aquifer drains slowly into the stream. Since we monitor simultaneously the stream discharge and the water table elevation, we may compare their evolution to the predictions of the Boussinesq approximation, and adjust the aquifer's hydraulic properties to fit the theory to our observations. During a dry period, the water table should decrease as the inverse of time, while the discharge of the stream decreases as the squared inverse of time (Brutsaert & Nieber, 1977). The Quiock aquifer accords with this theory (Supporting Information Text S6 and Figure S3), and we find a drainable porosity of $\phi_d \approx 5.3 \times 10^{-2}$, an ordinary value for clay (Batu, 1998). This analysis also yields another estimate for the hydraulic conductivity, $K \approx 4.1 \times 10^{-6}\,\mathrm{m\,s^{-1}}$, which is consistent with the estimate based on equation (1). These findings supports the assumption, so far unsubstantiated, that the permeability of the aquifer decreases quickly below the stream's level, and encourage us to use the non-linear Boussinesq equation during the early stage of a rainfall event as well. In the next section, we analyze our observations in search of the storm regime.

4 Storm-flow Regime

After a drought, the water table is low and the stream discharge recedes. The next rainfall event abruptly increases the groundwater pressure throughout the shallow aquifer, which responds by expelling more water into the neighboring stream. Following Guérin et al. (2014), we now idealize this scenario by considering an initially empty aquifer suddenly recharged at rate R_s. Under these assumptions, the groundwater flow enters the storm-flow regime of the Boussinesq equation, the mathematical expression of which was derived by Guérin et al. (2014) (Supporting Information Text S7). Here we propose a simpler derivation which better illuminates the mechanics of this peculiar regime, at the cost of mathematical rigour.

Figure 2 shows the theoretical shape of the water table as it swells to accommodate the rainfall input (Guérin et al., 2014). We now approximate this mathematical solution by splitting it into two connected regions. Far from the outlet, the water table rises at

velocity R_s/ϕ_f, unaffected by the groundwater lost to the stream. Meanwhile, a smooth front of length L_f connects the outlet to this rising plateau. Along this front, the water table is virtually at equilibrium with the recharge. Since, in this simple reasoning, the rising plateau delivers no water to the front, the groundwater discharge per unit length of stream is $R_s L_f$—collected entirely by the front. The front's shape is that of a steady water table in an aquifer of length L_f, that is, equation (1) in which we substitute $\langle R \rangle$ with R_s, and L_a with L_f. However, the front is not exactly at equilibrium, since it needs to match the height of the rising plateau; this requires that the front's thickness increase linearly with time, according to $L_f = \sqrt{K R_s}\, t/\phi_f$, where t is the time elapsed since the beginning of recharge. This matching yields the approximate shape of the water table in the storm-flow regime (red lines in Figure 2). Although not rigorous, this procedure yields the same expression as Guérin et al. (2014), but for a prefactor of order one.

Unfortunately, in the Quiock catchment, the spatial resolution of our water-table measurements does not allow for a direct comparison between the actual water table and the solution derived above. Indeed, after one hour of sustained and intense rainfall, we expect the equilibrium front to extend over a few meters only (Figure 2). Instead, we may calculate the amount of groundwater the aquifer delivers to the stream during a rainfall event, and compare it to the associated discharge surge we measure in the stream, ΔQ_s. To do so, we first derive the groundwater flow that exits the aquifer in the storm regime at time T_s (Supporting Information Text S7):

$$\Delta Q_s \approx 2 L_r \frac{\sqrt{K}}{\phi_f} R_s^{3/2} T_s \,. \tag{3}$$

This expression is similar to the equation derived by Guérin et al. (2014), but for a numerical prefactor of about 0.73, which is accessible only to a thorough mathematical derivation of the storm-flow regime. As expected, we recover the exponent of 3/2 that distinguishes the storm-flow regime. The above equation also shows that the storm flow, like most asymptotic regimes in dissipative systems, does not depend on initial conditions (i.e. the shape of the water table before the rainfall event). How decent an approximation this mathematical feature will prove in practice is, at this point, open to question.

Equation (3) involves parameters that are sometimes difficult to measure (L_r, K and ϕ_f), and the recharge rate raised to a non-integer exponent—a quantity whose dimensions are hardly meaningful. To produce a more presentable version of Eq. (3), we divide it by the average water balance for the catchment, namely $\langle Q \rangle = A \langle R \rangle$. We thus get

$$\frac{\Delta Q_s}{\langle Q \rangle} \approx \frac{2\, L_r \sqrt{K \langle R \rangle}}{A\, \phi_f} \left(\frac{R_s}{\langle R \rangle} \right)^{3/2} T_s \,. \tag{4}$$

Finally, using Eq. (2) to express the characteristic time T_c of the aquifer in terms of the hydraulic properties of the latter, we rewrite Eq. (4) as:

$$\frac{\Delta Q_s}{\langle Q \rangle} = C \frac{T_s}{T_c} \left(\frac{R_s}{\langle R \rangle} \right)^{3/2} , \tag{5}$$

where $C \approx 0.57$ is the numerical prefactor derived by Guérin et al. (2014) (Supporting Information Text S7). The above equation is equivalent to Eq. (3), but perhaps more telling. Its advantages are that (i) all quantities are made non-dimensional using their average value, and (ii) the hydrological properties of the aquifer are all lumped into a single free parameter, the characteristic time T_c (or, equivalently, the available volume V_a). These advantages, however, come at a cost: the presence of average quantities ($\langle Q \rangle$, T_c and $\langle R \rangle$) in Eq. (5) might suggest that the prefactor of this power-law depends on the average hydrological conditions. In fact, however, a change in the average rainfall rate would affect $\langle Q \rangle$ and $T_c \langle R \rangle^{3/2}$ in the same proportion, and Eq. (5) would thus remain unaffected—so long as the groundwater flow has entered the storm-flow regime.

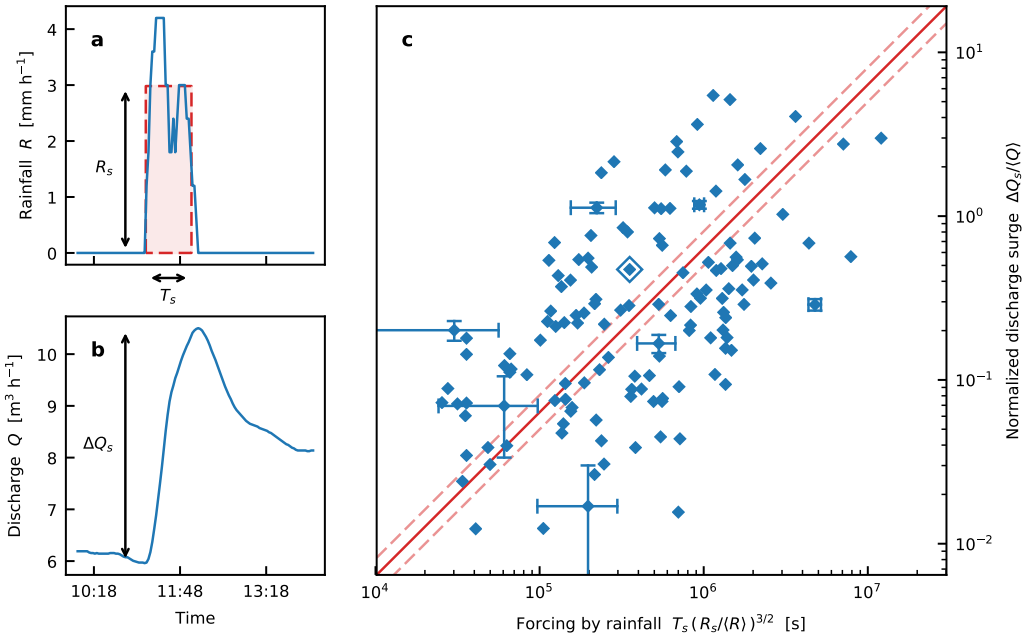

Figure 3. Relationship between rainfall intensity and associated surge in the stream discharge. (a) Rainfall event. Blue line shows actual time series superimposed over its mathematical representation (red dashed rectangle). The rectangle's area, $R_s\,T_s$, and duration, T_s, are the integral and variance of the actual signal, respectively. (b) Surge of stream discharge caused by the rainfall event of panel A, with amplitude ΔQ_s. (c) Normalized discharge surge, $\Delta Q_s/\langle Q \rangle$, as a function of the product of the duration of the rainfall event, T_s, with the normalized rainfall intensity, $R_s/\langle R \rangle$, to the power 3/2 for 137 isolated rainfall events between January 2015 and October 2017. Error bars indicate measurement error (Supporting Information Text S3). Only a few error bars, selected for representativity, are shown. Rimmed marker indicates event of panels A and B. Solid red line shows proportionality (equation (5) with $T_c = 10.4$ days). Dashed red lines represent the standard deviation of T_c in logarithmic space.

We now compare the storm-flow regime with our field measurements. Let us consider a rainfall event such as the one of Figure 3a, which we idealize with a constant recharge rate R_s over a time T_s (Supporting Information Text S3). The aquifer responds to this input by delivering more water to the stream, the discharge of which thus surges (Figure 3b). Assuming that this surge is due mostly to the groundwater input, we can measure ΔQ_s on the hydrograph of the Quiock stream (Supporting Information Text S3), and normalize it with $\langle Q \rangle$, the average stream discharge. We now wish to compare this relative discharge surge to the storm-flow regime, embodied by Eq. (3). In doing so, we assume that the aquifer, or at least its shallower, most reactive part is virtually empty before the rainfall event. This, strictly speaking, is not true unless the stream dries out entirely. Still, this approximation can hold when the water table has enough time to recede between two rainfall events, but it is unlikely to hold when rains quickly follow each other.

Between January 2015 and October 2017, we have identified 137 isolated rainfall events, and measured the associated discharge surge ΔQ_s, rainfall intensity R_s, and total volume of water delivered to the catchment V_s (Supporting Information Text S3). Figure 3 shows these measurements in the coordinates suggested by equation (5), namely the normalized discharge surge $\Delta Q_s/\langle Q \rangle$, and the product of the rainfall duration, T_s, with the power 3/2

of the normalized rainfall intensity, $R_s/\langle R\rangle$, measured as shown on Figs. 3**a** and **b**. Both quantities spread over almost three orders of magnitude, revealing a positive correlation (the Pearson coefficient is 0.55 in logarithmic space), despite a significant scatter (about one order of magnitude). Fitting a power law to our data by orthogonal distance regression yields an exponent of 0.98 ± 0.09, close to the exponent of one predicted by equation (5). Assuming this exponent is indeed one, we find that a characteristic time of $T_c \approx 10.4\,\text{days}$ best fits our data, which corresponds to an available volume of $V_a \approx 2\,400\,\text{m}^3$. We thus find that the fillable porosity is about $\phi_f \approx 1.3 \times 10^{-2}$, a value less than a fourth of the drainable porosity ϕ_d, as measured based on the recession flow—not a surprizing observation (Acharya et al., 2012). These values however, should be treated with caution, as they inherit the uncertainty associated to the dispersion of the data in Figure 3 (at least a factor of 5).

Among the many hypotheses that allow one to derive equation (5), the existence (and location) of a horizontal impervious layer below the stream's level is arguably the least substantiated. If, for comparison, we assume that such a layer lies a few meters below the stream's level, the groundwater flow would not enter the storm-flow regime. Instead, we would expect it to enter the linear counterpart of this assymptotic behavior (provided the Boussinesq approximation still holds), and the stream's discharge would then increase like $R_s\sqrt{T_s}$ (Pauwels & Troch, 2010; Pauwels & Uijlenhoet, 2019). Despite the scatter of Figure 3, there is little doubt that this linear regime does not fit our observations, thus supporting, in retrospect, the assumption of a fully-penetrating stream. Still, this simplifying hypotheses can only be a crude model of the Quiock aquifer, the actual geometry of which probably contributes to the dispersion of the data around the storm regime.

Often, the volume of groundwater that a catchment contains affects its response to the rainfall signal. This sensitivity to initial conditions could also explain part of the dispersion in Figure 3 (Biswal & Nagesh Kumar, 2014; Botter, Porporato, Rodriguez-Iturbe, & Rinaldo, 2009; Kirchner, 2009). Indeed, we may only expect the storm-flow regime to be a decent representation of the groundwater flow if the aquifer is essentially empty before the rainfall event. (Even in the framework of the Boussinesq approximation, the initial shape of the water table influences the response of the groundwater flow to recharge.) To evaluate the state of the groundwater flow before a rainfall event, we measure the discharge Q_i of the stream just before it rises, for the 137 events of Figure 3 (Supporting Information Text S8). Surprisingly, once detrended according to equation (5), the response of the stream's discharge appears uncorrelated with the ratio $Q_i/\Delta Q_s$, even when the latter becomes larger than one—that is, when we would expect the storm-flow regime to break down (Supporting Information Figure S4**a**). A different picture emerges if we normalize the initial discharge with the average discharge of the stream ($Q_i/\langle Q\rangle$ then becomes our proxy for the groundwater's state, Supporting Information Figure S4**b**). The prefactor of equation (5) increases significantly with this ratio, showing the influence of initial conditions on the groundwater's response to rainfall events, but this correlation disappears for the most isolated events ($Q_i/\langle Q\rangle$ less than about 0.1). Repeating this analysis with the elevation of the water table in piezometer G confirms these observations, although with a lesser statistical significance (Supporting Information Figure S4**c** and S4**d**).

It is remarkable that the power-law relation associated to the storm-flow regime appears to hold even for rainfall events that are not, strictly speaking, isolated from the previous ones—although such events probably cause some of the scatter visible in Figure 3. If we restrict the analysis to the most isolated rainfall events, thus reducing our data set to only ten points, we find that a critical time of $T_c \approx 49\,\text{days}$ best fits our observations (Supporting Information Text S8). Although less significant statistically, this value might be more relevant physically. If so, the available volume of water in the catchment would be closer to $V_a \approx 11\,000\,\text{m}^3$, and the associated fillable porosity would be $\phi_f \approx 6.0 \times 10^{-2}$—very close to the drainable porosity.

5 Conclusion

Like most field observations, our measurements are highly variable, and the Boussinesq approximation can only provide a rudimentary model of the groundwater dynamics during a rainfall event. Even where this approximation is appropriate, we can only expect the storm-flow regime to occur during rainfall events that are isolated from previous ones. Nonetheless, this regime expresses itself unambiguously in the hydrograph of the Quiock Creek, thus displaying the typical robustness of asymptotic regimes (Barenblatt, 1996). Among the rainfall events we have identified over 3 years, only a few qualify as floods—none of them catastrophic. The trend shown on Fig. 3c, however, shows no sign of abating, and the scaling law of the storm-flow regime might fit more severe events than those of our data set.

We suggest that the storm-flow regime takes place in many catchments where groundwater flows through a shallow unconfined aquifer. It would thus contribute to the widespread non-linearity of small catchments (Botter et al., 2009; Buttle, Dillon, & Eerkes, 2004; Kirchner, 2009; Tromp-van Meerveld & McDonnell, 2006; Uchida, Tromp-van Meerveld, & McDonnell, 2005). Of course, we would need more high-frequency rainfall and discharge measurements to support this hypothesis. Provided such time series, the plot of Figure 3 makes it straightforward to calibrate equation (5), which in turn can be implemented either as a source term in watershed models (Thompson, Sørenson, Gavin, & Refsgaard, 2004), or included in low-dimensional, physically-based models of the groundwater dynamics (Basso, Schirmer, & Botter, 2016; Kirchner, 2009). We trust this could improve flood forecasting in catchments dominated by shallow groundwater. In addition, the calibration of equation (5) yields the average volume of groundwater, V_a, that a catchment stores above the stream level—an estimate of the amount of water that will be released during a prolonged drought.

Finally, as a solution of the non-linear Boussinesq equation, the storm-flow regime reconciles the classical drought flow with the quick response of groundwater to rainfall. This encouraging finding bolsters the renewed interest in Boussinesq's theory that high-frequency measurement devices have fostered (Troch et al., 2013).

Acknowledgments

All the time series used in this paper were collected by the *Observatoire de l'eau et de l'érosion aux Antilles* (ObsERA, INSU-CNRS). They are available at `http://webobsera.ipgp.fr/`. We thank the members of the *Observatoire Volcanologique et Sismologique de Guadeloupe*, and specially O. Crispi, for technical support. We are grateful to the *Parc National de la Guadeloupe*, and specially to S. La Pierre de Melinville and M. Gombauld, for granting us access to the field site. We thank S. Basso for suggesting, during the review process, to introduce the characteristic time of equation (5).

References

Abdul, A., & Gillham, R. (1984). Laboratory studies of the effects of the capillary fringe on streamflow generation. *Water Resources Research*, *20*(6), 691–698.

Abdul, A., & Gillham, R. (1989). Field studies of the effects of the capillary fringe on streamflow generation. *Journal of Hydrology*, *112*(1-2), 1–18.

Acharya, S., Jawitz, J. W., & Mylavarapu, R. S. (2012). Analytical expressions for drainable and fillable porosity of phreatic aquifers under vertical fluxes from evapotranspiration and recharge. *Water Resources Research*, *48*(11).

Barenblatt, G. I. (1996). *Scaling, self-similarity, and intermediate asymptotics: dimensional analysis and intermediate asymptotics* (Vol. 14). Cambridge University Press.

Basso, S., Schirmer, M., & Botter, G. (2016). A physically based analytical model of flood frequency curves. *Geophysical Research Letters*, *43*(17), 9070–9076.

Batu, V. (1998). *Aquifer hydraulics: a comprehensive guide to hydrogeologic data analysis* (Vol. 1). John Wiley & Sons.

Berkowitz, B. (2002). Characterizing flow and transport in fractured geological media: A review. *Advances in water resources*, *25*(8), 861–884.

Beven, K. (1981). Kinematic subsurface stormflow. *Water Resources Research*, *17*(5), 1419-1424.

Beven, K., & Germann, P. (1982). Macropores and water flow in soils. *Water resources research*, *18*(5), 1311-1325.

Biswal, B., & Nagesh Kumar, D. (2014). Study of dynamic behaviour of recession curves. *Hydrological Processes*, *28*(3), 784–792.

Botter, G., Porporato, A., Rodriguez-Iturbe, I., & Rinaldo, A. (2009). Nonlinear storage-discharge relations and catchment streamflow regimes. *Water resources research*, *45*(10).

Boussinesq, J. (1904). Recherches théoriques sur l'écoulement des nappes d'eau infiltrées dans le sol et sur le débit des sources. *Journal de mathématiques pures et appliquées*, 5-78.

Brutsaert, W., & Nieber, J. L. (1977). Regionalized drought flow hydrographs from a mature glaciated plateau. *Water Resources Research*, *13*(3), 637-643.

Buss, H. L., White, A. F., Dessert, C., Gaillardet, J., Blum, A. E., & Sak, P. B. (2010). Depth profiles in a tropical volcanic critical zone observatory: Basse-terre, guadeloupe. In *Proc. of the 13th intl. symp. on water–rock interaction.*

Buttle, J. M., Dillon, P. J., & Eerkes, G. R. (2004, feb). Hydrologic coupling of slopes, riparian zones and streams: an example from the canadian shield. *Journal of Hydrology*, *287*(1), 161-177. doi: 10.1016/j.jhydrol.2003.09.022

Cardenas, M. B. (2007). Potential contribution of topography-driven regional groundwater flow to fractal stream chemistry: Residence time distribution analysis of tóth flow. *Geophysical Research Letters*, *34*(5).

Clergue, C., Dellinger, M., Buss, H. L., Gaillardet, J., Benedetti, M. F., & Dessert, C. (2015). Influence of atmospheric deposits and secondary minerals on li isotopes budget in a highly weathered catchment, guadeloupe (lesser antilles). *Chemical Geology*, *414*, 28-41. doi: 016/j.chemgeo.2015.08.015

Cloke, H., Anderson, M., McDonnell, J., & Renaud, J.-P. (2006). Using numerical modelling to evaluate the capillary fringe groundwater ridging hypothesis of streamflow generation. *Journal of Hydrology*, *316*(1-4), 141–162.

Colmet-Daage, F., & Lagache, P. (1965). Caractéristiques de quelques groupes de sols dérivés de roches volcaniques aux antilles françaises. *Cahiers de l'ORSTOM serie pédologie*, *8*, 91-121.

De Marsily, G., Delay, F., Goncalves, J., Renard, P., Teles, V., & Violette, S. (2005). Dealing with spatial heterogeneity. *Hydrogeology Journal*, *13*(1), 161–183.

Dupuit, J. (1848). *Etudes theoriques et pratiques sur le mouvement des eaux courantes.* Carilian-Goeury.

Fiori, A. (2012). Old water contribution to streamflow: Insight from a linear boussinesq model. *Water Resources Research*, *48*(6).

Fiori, A., Romanelli, M., Cavalli, D., & Russo, D. (2007). Numerical experiments of streamflow generation in steep catchments. *Journal of hydrology*, *339*(3-4), 183–192.

Goderniaux, P., Davy, P., Bresciani, E., Dreuzy, J.-R., & Le Borgne, T. (2013). Partitioning a regional groundwater flow system into shallow local and deep regional flow compartments. *Water Resources Research*, *49*(4), 2274–2286.

Guérin, A., Devauchelle, O., & Lajeunesse, E. (2014, nov). Response of a laboratory aquifer to rainfall. *Journal of Fluid Mechanics*, *759*, -1. doi: 10.1017/jfm.2014.590

Harman, C., & Sivapalan, M. (2009). A similarity framework to assess controls on shallow subsurface flow dynamics in hillslopes. *Water Resources Research*, *45*(1), n/a–n/a. Retrieved from `http://dx.doi.org/10.1029/2008WR007067` (W01417) doi: 10.1029/2008WR007067

Jasechko, S., Kirchner, J. W., Welker, J. M., & McDonnell, J. J. (2016, feb). Substantial proportion of global streamflow less than three months old. *Nature Geoscience*, *9*, 126-129. doi: 10.1038/NGEO2636

Kirchner, J. W. (2003). A double paradox in catchment hydrology and geochemistry. *Hydrological Processes*, *17*(4), 871-874. doi: 10.1002/hyp.5108

Kirchner, J. W. (2009). Catchments as simple dynamical systems: Catchment characterization, rainfall-runoff modeling, and doing hydrology backward. *Water Resources Research*, *45*(2), n/a–n/a. Retrieved from `http://dx.doi.org/10.1029/2008WR006912` (W02429) doi: 10.1029/2008WR006912

Maher, K., DePaolo, D. J., Conrad, M. E., & Serne, R. J. (2003). Vadose zone infiltration rate at hanford, washington, inferred from sr isotope measurements. *Water Resources Research*, *39*(8).

Mares, R., Barnard, H. R., Mao, D., Revil, A., & Singha, K. (2016). Examining diel patterns of soil and xylem moisture using electrical resistivity imaging. *Journal of Hydrology*, *536*, 327–338.

McDonnell, J. J. (1990). A rationale for old water discharge through macropores in a steep, humid catchment. *Water Resources Research*, *26*(11), 2821-2832.

McDonnell, J. J. (2003, jun). Where does water go when it rains?: Moving beyond the variable source area concept of rainfall-runoff response. *Hydrological processes*, *17*(9), 1869-1875. doi: 10.1002/hyp.5132

McDonnell, J. J., McGuire, K., Aggarwal, P., Beven, K. J., Biondi, D., Destouni, G., ... others (2010). How old is streamwater? open questions in catchment transit time conceptualization, modelling and analysis. *Hydrological Processes*, *24*(12), 1745–1754.

McGlynn, B. L., McDonnel, J. J., & Brammer, D. D. (2002). A review of the evolving perceptual model of hillslope flowpaths at the maimai catchments, new zealand. *Journal of Hydrology*, *257*(1-4), 1–26.

McKay, L. D., Driese, S. G., Smith, K. H., & Vepraskas, M. J. (2005). Hydrogeology and pedology of saprolite formed from sedimentary rock, eastern tennessee, usa. *Geoderma*, *126*(1-2), 27–45.

Montgomery, D. R., Dietrich, W. E., Torres, R., Anderson, S. P., Heffner, J. T., & Loague, K. (1997). Hydrologic response of a steep, unchanneled valley to natural and applied rainfall. *Water Resources Research*, *33*(1), 91–109.

Neal, C., & Rosier, P. T. (1990). Chemical studies of chloride and stable oxygen isotopes in two conifer afforested and moorland sites in the british uplands. *Journal of Hydrology*, *115*(1-4), 269–283.

Park, E., & Parker, J. (2008). A simple model for water table fluctuations in response to precipitation. *Journal of Hydrology*, *356*(3-4), 344–349.

Pauwels, V. R. N., & Troch, P. A. (2010). Estimation of aquifer lower layer hydraulic conductivity values through base flow hydrograph rising limb analysis. *Water resources research*, *46*(3). doi: 10.1029/2009WR008255

Pauwels, V. R. N., & Uijlenhoet, R. (2019). Confirmation of a short-time expression for the hydrograph rising limb of an initially dry aquifer using laboratory hillslope outflow experiments. *Water Resources Research*, *0*(0). Retrieved from `https://agupubs.onlinelibrary.wiley.com/doi/abs/10.1029/2018WR023580` doi: 10.1029/2018WR023580

Rupp, D. E., Schmidt, J., Woods, R. A., & Bidwell, V. J. (2009). Analytical assessment and parameter estimation of a low-dimensional groundwater model. *Journal of hydrology*, *377*(1-2), 143–154.

Sanchez-Vila, X., Guadagnini, A., & Carrera, J. (2006). Representative hydraulic conductivities in saturated groundwater flow. *Reviews of Geophysics*, *44*(3).

Schoeneberger, P., & Amoozegar, A. (1990). Directional saturated hydraulic conductivity and macropore morphology of a soil-saprolite sequence. *Geoderma*, *46*(1-3), 31–49.

Sefton, C., Whitehead, P., Eatherall, A., Littlewood, I., & Jakeman, A. (1995). Dynamic response characteristics of the plynlimon catchments and preliminary analysis of relationships to physical descriptors. *Environmetrics*, *6*(5), 465–472.

Sidle, R. C., Tsuboyama, Y., Noguchi, S., Hosoda, I., Fujieda, M., & Shimizu, T. (2000). Stormflow generation in steep forested headwaters: a linked hydrogeomorphic paradigm. *Hydrological Processes*, *14*(3), 369-385.

Sklash, M. (1990). Environmental isotope studies of storm and snowmelt runoff generation. *Process studies in hillslope hydrology*, 401–436.

Sklash, M. G., & Farvolden, R. N. (1979). The role of groundwater in storm runoff. *Developments in Water Science*, *12*, 45-65.

Sophocleous, M. A. (1991). Combining the soilwater balance and water-level fluctuation methods to estimate natural groundwater recharge: practical aspects. *Journal of hydrology*, *124*(3-4), 229–241.

Tani, M. (1997). Runoff generation processes estimated from hydrological observations on a steep forested hillslope with a thin soil layer. *Journal of Hydrology*, *200*(1), 84-109.

Thompson, J., Sørenson, H. R., Gavin, H., & Refsgaard, A. (2004). Application of the coupled mike she/mike 11 modelling system to a lowland wet grassland in southeast england. *Journal of Hydrology*, *293*(1), 151–179.

Toth, J. (1963). A theoretical analysis of groundwater flow in small drainage basins. *Journal of geophysical research*, *68*(16), 4795–4812.

Troch, P. A., Berne, A., Bogaart, P., Harman, C., Hilberts, A. G., Lyon, S. W., ... others (2013). The importance of hydraulic groundwater theory in catchment hydrology: The legacy of wilfried brutsaert and jean-yves parlange. *Water Resources Research*, *49*(9), 5099–5116.

Tromp-van Meerveld, H., & McDonnell, J. (2006). Threshold relations in subsurface stormflow: 2. the fill and spill hypothesis. *Water Resources Research*, *42*(2).

Uchida, T., Tromp-van Meerveld, I., & McDonnell, J. J. (2005, sep). The role of lateral pipe flow in hillslope runoff response: an intercomparison of non-linear hillslope response. *Journal of Hydrology*, *311*(1), 117-133. doi: 10.1016/j.jhydrol.2005.01.012